

Uncertainties in passive seismic monitoring

Leo Eisner¹, Werner M. Heigl², Peter M. Duncan¹, William R. Keller³

¹ Microseismic Inc, Houston, TX, USA

² Apache, Houston, TX, USA

³ Chesapeake Energy, Oklahoma City, OK, USA

The use of passive seismic techniques to monitor oil field completion and production processes is on the rise. Stress changes induced by such reservoir activities as hydraulic fracturing, water injection or fluid extraction will often result in failure of the rocks with a concurrent release of seismic energy in the form of compressional (p) and shear (s) waves. Passive seismic monitoring is based on recording these emitted waves and then using their arrival times to estimate the location of the failure events.

The distribution of event locations in time and space can then be used to deduce how the reservoir rocks are responding to the production activity. Such information, coupled with other ongoing measurements of fluid temperature and pressure, make an essential contribution to the "smart oilfield". An understanding of the uncertainties in these event locations is essential to a proper employment of the technology.

A microseismic event occurs at an unknown origin time and at an unknown location, or hypocenter. Because p and s waves travel at different velocities, the distance from the hypocenter to a single receiver may be estimated by observing the differential arrival times of the p and s wave phases at that receiver location. Given a sufficiently widely distributed array of at least three sensors, an estimate of the hypocenter location may be made through the process of trilateration. Using 3-component phones such that the polarization of the event arrival and therefore wavefront propagation direction may be determined, allows for an additional constraint on the location estimate. This constraint is useful and perhaps even necessary in limited aperture situations such as when the sensor array is deployed in a monitoring borehole. However, microseisms caused by slip along an induced or

pre-existing fracture plane do not radiate energy equally in all directions (reference figure 1B). In fact, this type of radiation pattern includes two nodal planes along which little or no seismic energy of the particular phase is received. It follows that if a downhole monitoring array were located along the nodal plane of such an event, the event would not be detected.

In this study, we investigate uncertainties in the estimated locations of microseismic events given various receiver array geometries. We illustrate how these errors are affected by the location of the receiver array, focusing on two that are commonly applied in practice: a 2-D grid of receivers on the earth's surface and a linear array of receivers in a single vertical borehole. We also present a limited analysis of location errors due to an incorrect velocity in a homogeneous medium. However, we recognize that velocity heterogeneity may have an equally profound effect on location accuracy as receiver distribution.

How are event locations determined?

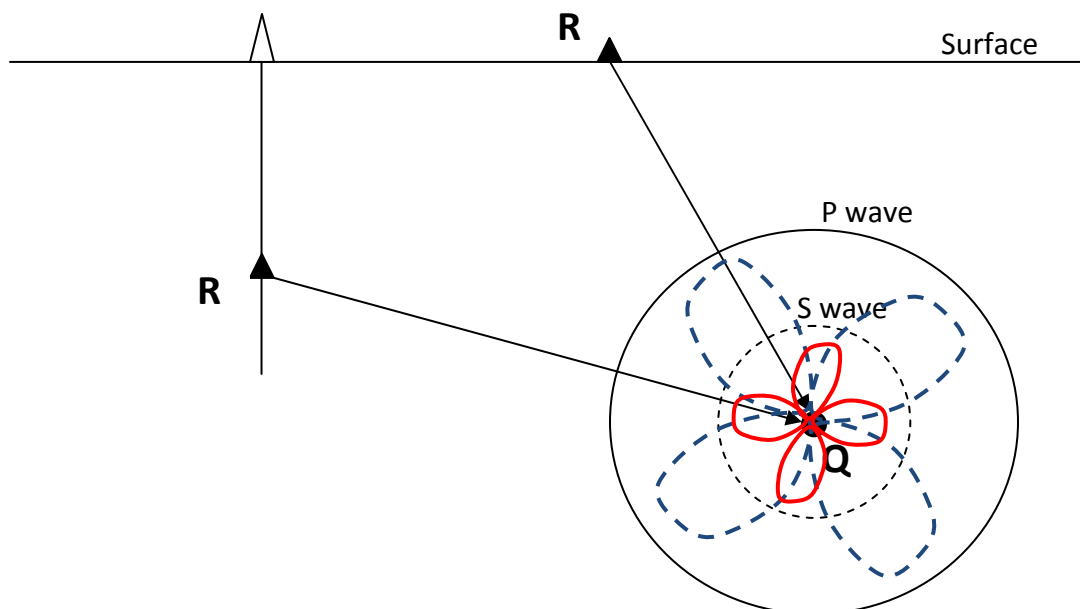


Figure 1: A micro-seismic event at Q generates P and S waves that travel through the medium and, after some time, arrive at sensors located at R. This sensor is typically on the earth's surface or on a

downhole wireline tool. Red and blue curves illustrate an example of possible amplitude radiation pattern from P- and S-waves, respectively (i.e., S-to-P-wave amplitude is proportional to the cube of P-to-S-wave velocity ratio).

Figure 1 illustrates the geometry of the experiment assuming a simple isotropic, homogeneous medium. A microseismic event occurs with an origin time (t_0) with a hypocenter location (Q). At arrival times t_p and t_s the p and s-waves are recorded at the receiver located at R. The P-wave arrives first at time:

$$t_p = t_0 + \Delta t_p$$

The S-wave arrives at a later time:

$$t_s = t_0 + \Delta t_s.$$

Δt_p and Δt_s denote traveltimes of P- and S-waves. Noting that the distance QR is equal to traveltime multiplied by velocity, the above equations can be solved for distance:

$$\overline{QR} = (t_p - t_0)V_p = (t_s - t_0)V_s$$

At this point, surface and downhole methodologies diverge. Because of the noisy conditions in which surface microseismic data is recorded, a large, redundant array of thousands of geophones is deployed, and only P-wave arrival times are consistently imaged. P-wave arrival times are imaged across the array with a grid search through all possible subsurface event locations and origin times until the observed arrival time distribution is matched with synthetic traveltimes. This process is then repeated for subsequent events.

In the downhole case, the receiver array is constrained by physical and operational limitations associated with downhole wireline tools. As such, the downhole receiver array has a limited aperture with a small number of three component geophones. However, the quiet downhole environment allows accurate P and S-wave arrival times to be picked. Given the differential traveltime between the P and S-wave associated with a given event, the distance QR can be calculated.

$$\overline{QR} = (t_s - t_p) \left(\frac{1}{V_s} - \frac{1}{V_p} \right)^{-1} = (\Delta t_s - \Delta t_p) \left(\frac{1}{V_s} - \frac{1}{V_p} \right)^{-1}.$$

With typical downhole geophone array apertures, simple trilateration of event locations is not suitably accurate. As a result of this geometrical limitation, the azimuth of the arriving wavefronts must be used as an additional constraint to determine accurate microseismic event locations. The event azimuth may be determined directly from the p-wave because the particle polarization is parallel to the raypath direction for p-waves in an isotropic medium. For the accuracy of such measurement as well as S-wave backazimuth determination, see the recommended literature.

Sources of microseismic event uncertainty

The surface and downhole location techniques as described above work flawlessly in a homogeneous isotropic medium that is free of noise. In the real world, the wavefield propagating out from a microseismic event is complex, raypaths are bent by velocity heterogeneities, and the particle polarization used to estimate azimuth may not be linear. In addition, varying levels of background noise may complicate the accurate picking of P- and S-wave arrival times, a factor that is especially significant for surface microseismic monitoring. For most surface and downhole projects, velocities for P- and S-waves are derived from sonic logs recorded in a nearby well. Among other things, sonic log measurements are hampered by near borehole effects, anisotropy, and bandwidth limitations (sonic log bandwidth is usually more than an order of magnitude higher than seismic bandwidth). Downhole microseismic also requires the accurate measurement of event azimuth which in turn requires the accurate determination of the position and orientation of each receiver. Receiver position is calculated using a deviation survey, and receiver orientation is calculated with the use of calibration shots that are recorded when the borehole casing is perforated. Calibration to perforation shots is done under the assumption that the medium is laterally homogeneous and isotropic (or media with vertical axis of symmetry), and this assumption may also be a source of significant systematic error (see recommended literature).

All these factors contribute to uncertainty in the estimated event location, but it is difficult to quantify exactly how each of them affects the final location. In this study, we focus on how acquisition geometry, picking error in varying noise environments, and velocity model error may affect the accuracy of microseismic event locations. These are three important sources of error that are common to every microseismic experiment and thus should be understood by any geologist, geophysicist, or engineer who regularly uses and interprets microseismic data.

Graphical description of event location uncertainties

To highlight these sources of error for both surface and downhole measurements, we calculate probability density functions of event locations that are derived from relevant arrival times and azimuthal measurements assuming Gaussian distributions of errors. When plotted in color, these probability density functions are a useful way to graphically illustrate the event location uncertainty and how it can be described in 3D space. To simulate picking error and velocity model misfit, we calculate probability density function from realizations of arrival times and azimuths that have been perturbed by Gaussian noise with zero mean and a chosen standard deviation. The goal of this study is to graphically highlight certain patterns of systematic event location error so that the reader might identify and understand the cause of similar patterns in real-world datasets.

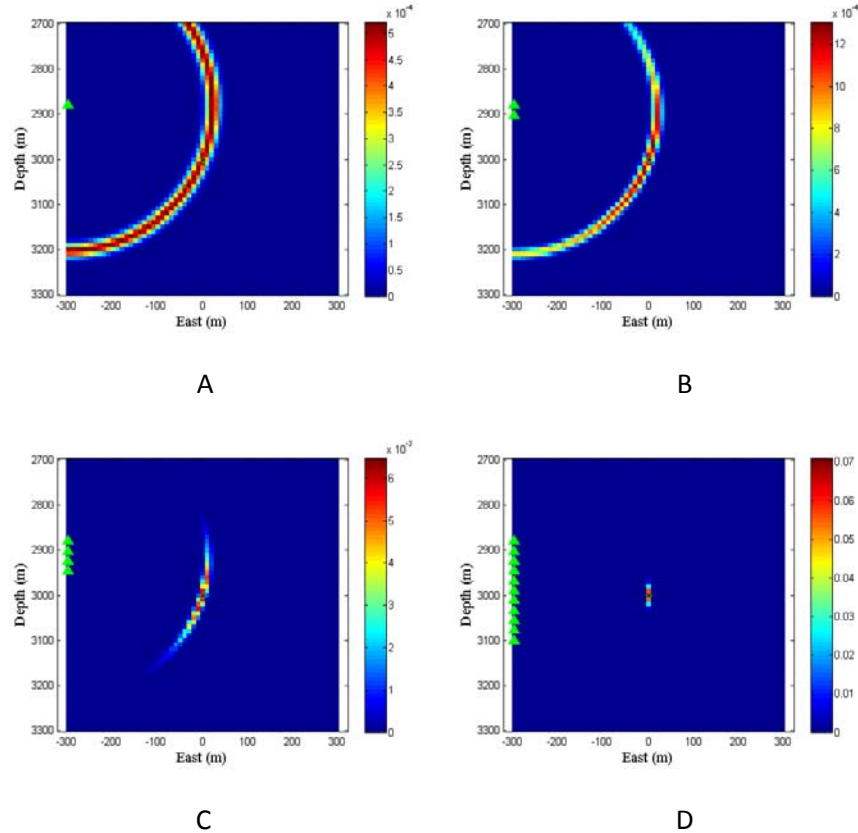


Figure 2. Vertical cross-sections through probability density functions (PDF) from 1 (plot A), 2 (B), 4 (C), and 11 (D) receivers in a single borehole and a microseismic event hypocenter located at the center of each plot (green circle). Hot colors show the most likely position of the located hypocenter. Decay from the hot to cold colors represents resolution and is determined by the acquisition geometry and the accuracy of the arrival times (assumed to be 1 ms). Each plot is normalized so that the probability density function sums to 1. The receivers are represented by green triangles on left side of each plot. Receiver spacing is 24 m and the maximum array spans 220 m vertically. P-wave and S-wave velocities are 5000 m/s and 3000 m/s, respectively.

Downhole microseismic monitoring

As discussed previously, a single receiver at which both arrival times of P- and S-wave are measured constrains only the distance, QR , from this receiver. Figure 2 illustrates how an array of geophones constrains depth and distance from a vertical well and was calculated with estimated pick uncertainty of 1 ms for arrival times of both P- and S-waves. We see this as a reasonable lower bound on pick uncertainty based on the results of Rutledge and Phillips (2003). In Figure 2, note that short

arrays (e.g., plot 1C geophones spanning 90 m) do not constrain the location very well. The location uncertainty is significantly reduced when receivers are located both above and below the event. Note that the resulting uncertainty in this cross-section from each array is largest in the vertical direction. This result is contrary to the common perception that depth is the best resolved coordinate from a vertical downhole array.

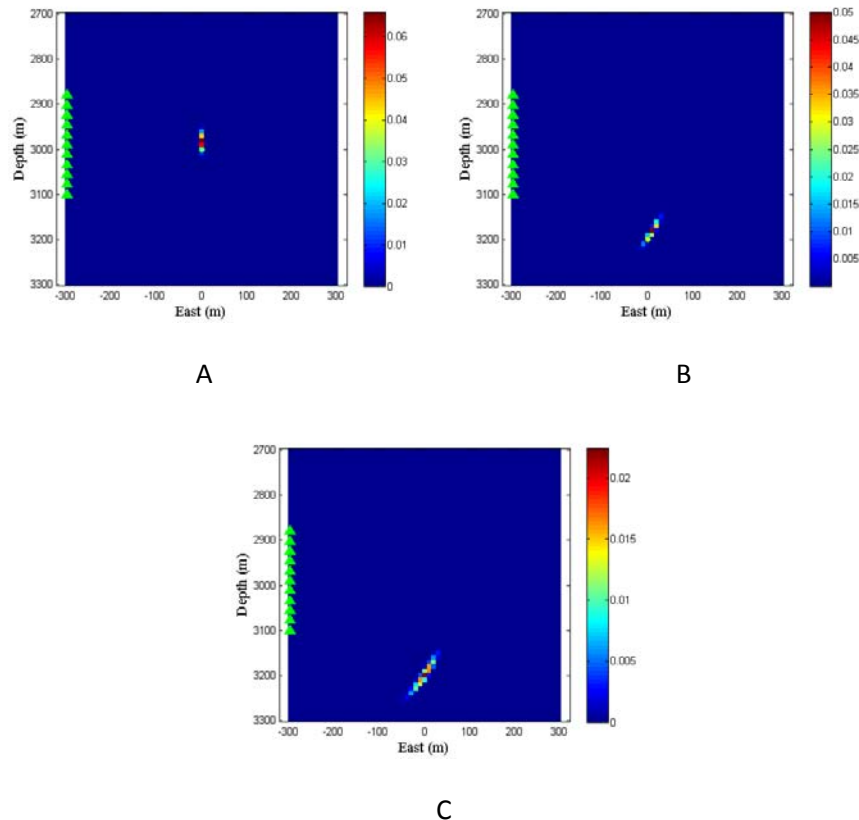


Figure 3. Vertical cross-sections through probability density functions (PDF) for events at various depths relative to the downhole receiver array. Plot A shows the PDF for a hypocenter located at a depth of the central receiver of the monitoring array. Plots B and C show the PDF for a hypocenter located below the borehole array (coordinates 0 and 3200 m). This is a very common scenario because wells are frequently plugged above the interval to be stimulated and receivers can't be lowered to minimize the location uncertainty. The arrival times of both P- and S-waves were perturbed with Gaussian random arrival time shifts of zero mean and 1 ms standard deviation. Plots A and B show one realization of this perturbation. Plot C shows an average PDF of 50 realizations of the Gaussian random arrival time shifts.

The shape of the event location uncertainty also depends on relative depth between the borehole array and the hypocenter. Figure 3 illustrates the shape of the uncertainty for two locations, one with a hypocenter depth directly in the center of the downhole receiver array (i.e., the same depth as in Figure 2) and one that is 80 m lower than the lowest receiver in the borehole array. This is a very common scenario because wells are frequently plugged above the interval to be stimulated and receivers can't be lowered to minimize the location uncertainty. Note that the probability density function of the deeper hypocenter is approximately twice as large and is tilted relative to the center of the array. To verify that this is not a result of a particular realization of the arrival time perturbation, we also show an average probability density function from 50 realizations of the arrival times and azimuths (plot 3C). This averaged probability density function from 50 realizations shows a larger uncertainty compared to the 1 realization case. The tilted axis of the probability density function may cause systematic errors in event distributions for events located deeper than the downhole array. For example, a series of repeated deep events with similar hypocenters but various noise dependent arrival times would locate along the shape of the PDF and could be interpreted as a dipping fault.

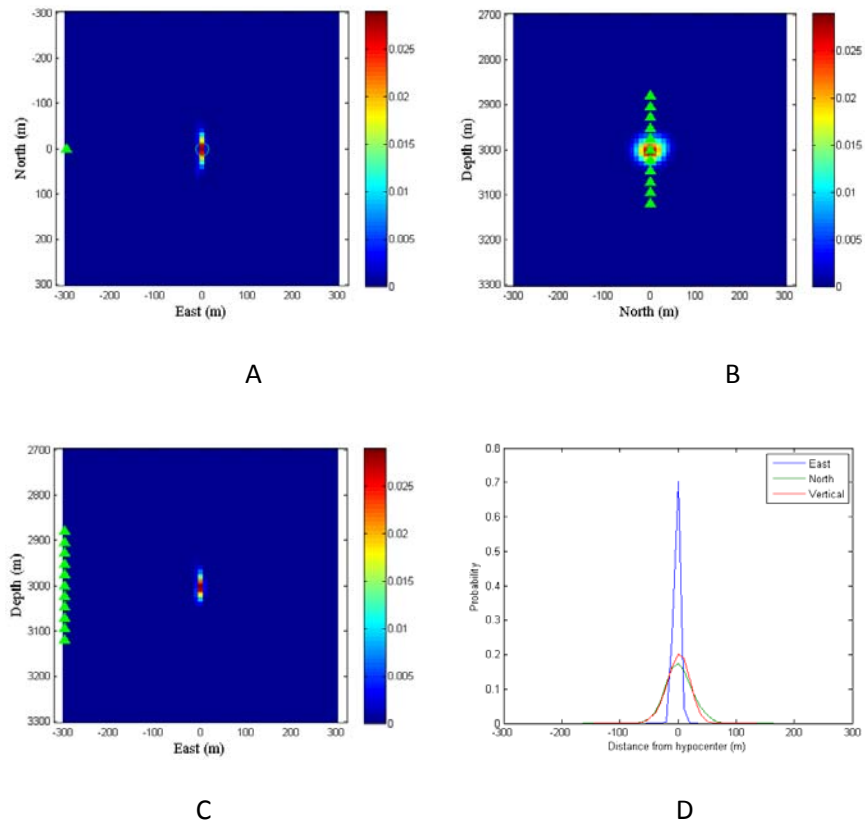


Figure 4. Three cross-sections through probability density functions of a hypocenter represented by the green circle located at east 0 m, north 0 m and depth 3000 m (4A - map view, 4B – N-S vertical cross-section, 4C – E-W vertical cross-section). Plot 4D shows integrated 1-D marginal pdfs. The receivers are represented by green triangles. Plots show 50 realizations of traveltimes and backazimuth measurements perturbed with Gaussian perturbation of standard deviation of 1 ms and 10° , respectively. For more details see Figure 1.

Figure 4 shows the true 3D uncertainty of a recorded microseismic event that includes lateral uncertainty resulting from particle polarization measurement. A Gaussian perturbation of azimuths with zero mean and a standard deviation of 10° was used in this calculation. This standard deviation was selected based on a recently published study by Fischer et al. (2008) who showed that a standard deviation of 10° and 15° is reasonable for S-wave and P-wave derived backazimuths respectively. Note that a more precise measurement of backazimuth may be possible for strong events recorded on a single receiver. However, the consistency of these azimuthal measurements across the borehole array is rather poor and significant discrepancies exist between P-wave and S-wave derived backazimuths.

In general, backazimuth measurements from particle polarization are more unstable than distance measurements derived from arrival time picks. This instability exists because particle polarization is sensitive to local velocity heterogeneity while travelttime measurements are the result of a cumulative integration along the entire raypath trajectory. As shown in Figure 4, the event location is most tightly constrained in the radial direction away from the borehole location. Depth and azimuth are much more poorly constrained. The relative values of the radial, azimuthal, and depth uncertainties may be best viewed in the 1-D histogram in plot 4D. For an average of 50 realizations, we calculated uncertainties in Cartesian coordinates of 5 m in the East (radial) direction, 23 m in the North (azimuthal) direction, and 20 m in the vertical direction. It is important to note that the length of the downhole array is one of the major factors that controls depth resolution. The density of receivers within the array does not reduce location uncertainty except in the case that nearby receivers are stacked to improve the signal-to-noise ratio. It is also worth noting that the uncertainties presented in Figure 4 are significantly higher than those provided by most service companies.

Surface microseismic monitoring

Microseismic events are typically recorded at the surface on large arrays of vertical component geophones distributed on the surface in a 2-D grid. For our calculations, we assume a surface array of 121 receivers organized in an 11 by 11 square grid with 600 m receiver spacing. As with downhole acquisition, receiver density does not influence the probability density function of the located hypocenters assuming a reasonable density of receivers, however stacking of seismograms is essential for overcoming low signal-to-noise ratios. The probability density function is primarily constrained by the aperture of the array relative to the event depth. For our calculations, we locate 3000 m deep events monitored from a 6000 by 6000 m array.

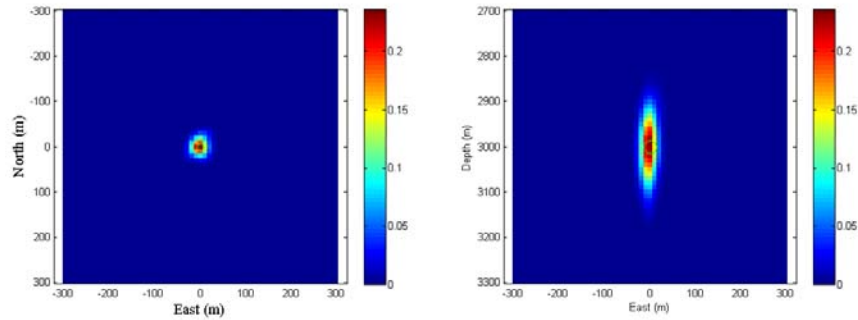


Figure 5. Two cross-sections through the 3-D probability density function of an event located at east and north 0 m and depth of 3000 m. The receiver array is an 11x11 square grid with 121 receivers. Event was located using only P-wave arrival times. P-wave arrival times were randomly perturbed with Gaussian distribution of zero mean and standard deviation of 10 ms. PDF represent an average of 45 realizations of these arrival times.

Figure 5 shows the probability density function of an event located using only P-wave arrival times recorded on the surface array. These arrival times were perturbed with Gaussian distribution of zero mean and standard deviation of 10 ms. The 10 ms uncertainty is considered as an upper bound and was derived from observed visible arrival times and their RMS. Recent datasets show an average RMS of 3.4 ms with receiver statics derived from a string shot. Surface monitoring has the added benefit of a more stable velocity model relative to downhole. Only the P-wave velocity model is required, and it can be constrained by sonic logs, a checkshot/VSP, or a 3D velocity model derived from surface 3D seismic acquisition. Receiver statics are an added source of uncertainty that have not been accounted for in this calculation, but they are typically very stable and do not vary with event hypocenter location. Note that the horizontal uncertainty is relatively well constrained with standard deviations of 14 m and 15 m in east and north direction respectively. On the other hand, vertical uncertainty is relatively poorly constrained with a standard deviation of 58 m. However, if we use 4 ms uncertainty in traveltimes corresponding to the measured RMS residuals, like we did for downhole measurement, the vertical error is reduced to 25 m and less than 10 m in horizontal directions.

Event uncertainties resulting from velocity model errors

A significant source of location uncertainty originates from the unknown subsurface velocity structure between the source and receivers. Because of differences in geometry, velocity errors affect event locations differently for surface and downhole monitoring. The top two plots in Figure 6 illustrate a simple downhole case for which the P-wave and S-wave velocities have been increased by 10% (plot 6A) and decreased by 10% (plot 6B). Given the asymmetry of the borehole monitoring array relative to the hypocenter location, the location error due to the velocity model affects both the horizontal and vertical location proportionally to the velocity error, i.e. the distance from the array is increased by approximately 10%. Note that the slower velocity appears to have much smaller uncertainty, thus giving a false indication of higher accuracy.

For surface microseismic monitoring, perturbations of the velocity model have a minimal effect on horizontal event uncertainties. However, these same perturbations have a very significant effect on depth related event uncertainties (bottom two plots in Figure 6), again approximately proportional to the distance of the event from the monitoring array. For the fast velocity model, the event is incorrectly located at a shallow depth. The opposite is true for the slow velocity model. However, it is interesting to note that the horizontal position of the located event is minimally affected even though the event is not located at the center of the surface monitoring array. The vertical error is overcome through calibration of the velocity model from perforation or check shot analogously to the conventional seismic time-to-depth conversion.

We note that the simple homogeneous velocity tests do not address the main difference between surface and downhole monitoring. In general the main factor is that the downhole monitoring uses waves propagating parallel to the horizontal bedding while surface monitoring is using waves travelling across the horizontal layers. Effects on locations are dependent on relative position of the monitoring borehole and velocity model and are case specific. Further reading can be found in recommended literature (e.g., Vesnaver et. al., 2008).

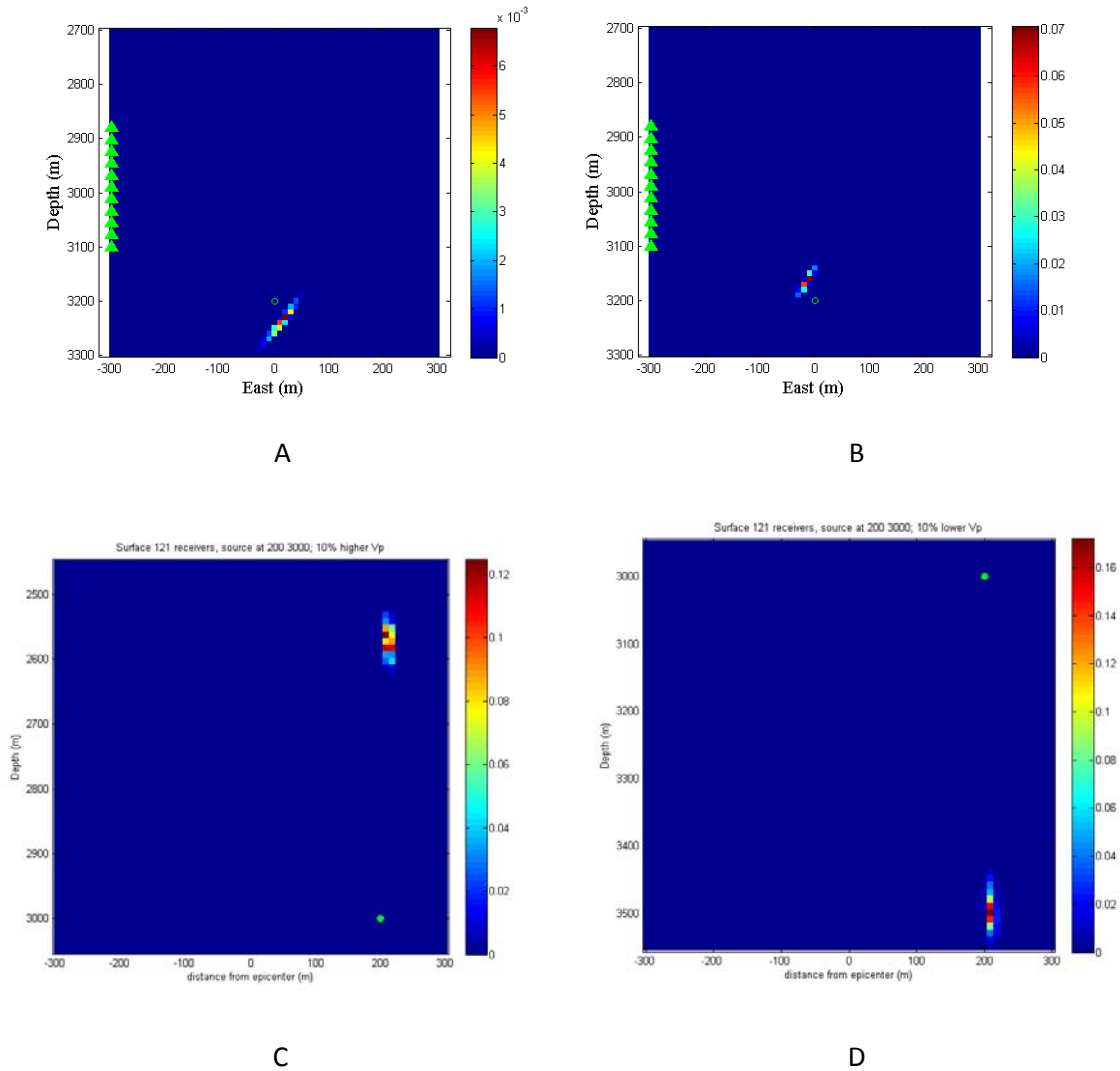


Figure 6: Four vertical cross-sections show velocity related location uncertainties for downhole monitoring (A and B) and surface monitoring (C and D). Plots A and C show a velocity model that is 10% faster and plots B and D show a velocity model that is 10% slower than the true velocity. All plots are shown at the same vertical and horizontal scale. For the downhole case, the arrival times were perturbed randomly with Gaussian distribution of zero mean and standard deviation of 1 ms for both P and S-waves. For the surface case, the arrival times were perturbed using a standard deviation of 4 ms for P-waves only. The true event location is represented with the green circle.

Location uncertainties for dual downhole arrays

An increasing number of microseismic monitoring jobs are using multiple monitoring wells to detect and locate microseismic events. In practice, a single microseismic event is rarely detected in more than two monitoring wells even if a field is instrumented with additional monitoring wells. This is likely due to the difficulties inherent in detecting events with such small magnitudes in combination

with many of the uncertainties described in the previous sections. In this section, we investigate the uncertainty related to a single microseismic event that is detected on two vertical downhole arrays of 11 geophones separated by 600 m.

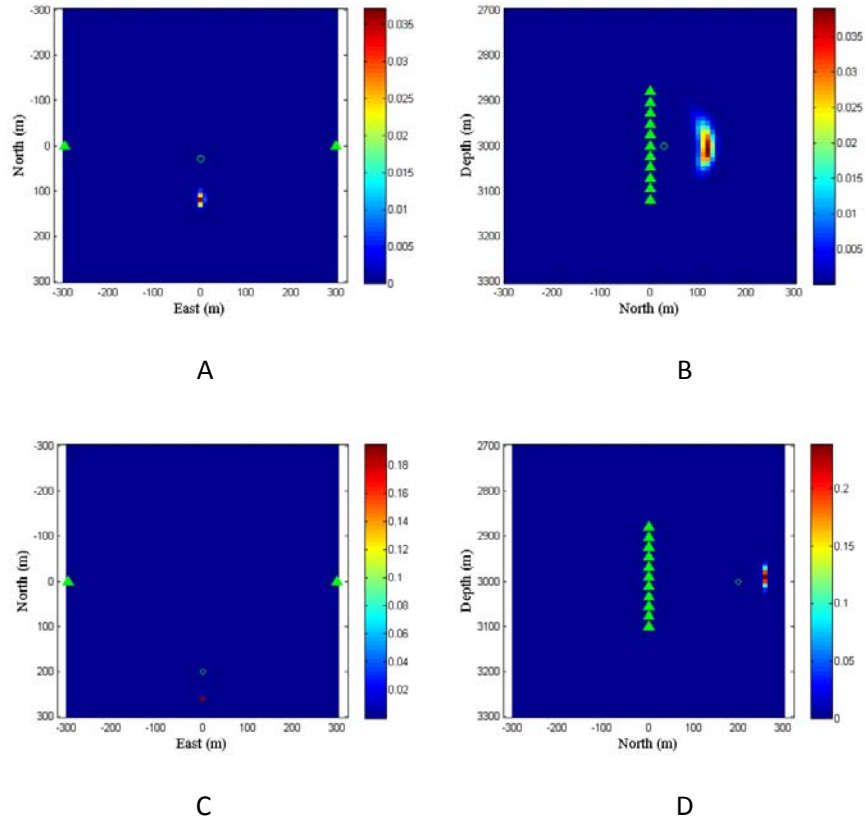


Figure 7: Dual borehole monitoring with incorrect (high) velocity model. Plots A and C show 2 map views at true hypocenter depths for locations derived from two monitoring vertical boreholes with 11 receivers each represented by the green triangles. Plots B and D show two vertical cross-sections through the true hypocenter (projected receiver positions are again represented by the green triangles). The true source position is represented by the green circle in each plot. Arrival times and backazimuths were perturbed randomly with Gaussian distribution of zero mean and standard deviation of 1 ms of both P and S-waves and 10° , respectively and the probability density functions represent an average of 50 realizations of these perturbations.

The top two plots in Figure 7 show the probability density function for an event located relatively close (30 m) to the plane of symmetry that connects the two monitoring wells. In this plot, the plane of symmetry is a horizontal line connecting the two wells in map view (top left plot in Figure 7). The bottom two plots in Figure 7 show the uncertainty related to an event that is relatively far away (200 m) from the plane of symmetry between the two wells. Intuitively, one might think

that the most accurate locations would occur between the two wells. However, Figure 7 clearly illustrates that the location close to the plane of symmetry between the wells is more poorly constrained than the event farther away from the plane of symmetry. Perhaps the most surprising illustration is shown in the right two plots which highlight the vertical uncertainty for the two events. The event far away from the plane of symmetry is much better constrained vertically than the event close to the plane of symmetry. In practice, linear clusters of event locations are often observed perpendicular to the plane of symmetry between dual monitoring wells. It is important to note that linear “trends” such as these may be geometrical artifacts that have nothing to do with fracture orientations.

Discussion

In this study, we have highlighted several common sources of error related to the location of microseismic events using both surface and downhole arrays (Table 1). For the downhole arrays, we characterize several unusual sources of systematic error that arise from the experiment geometry. These errors are often not intuitively obvious because geophysicists are accustomed to acquisition geometries in which both sources and receivers are located at the surface (neither of which is the case for downhole microseismic monitoring). For downhole microseismic monitoring, the most accurate event locations are obtained when the depth of the located event occurs within the depth range of the monitoring array with an aperture comparable to the event distance (Figures 2 and 3). Therefore, the array should straddle the zone of interest whenever possible and the array should span the expected depth range of recorded microseismic events. Contrary to common perception, we show that the depth of microseismic events recorded on a downhole array is much more poorly constrained than the radial distance from the borehole (Figures 2 and 4) assuming correct inversion model. In addition, we illustrated in Figures 3b and 3c that uncertainties for events located deeper than the downhole array are smeared along an inclined trend that may easily be misinterpreted as fault or fracture planes. Geophysicists typically think of velocity errors in terms of their affect on depth estimations. In Figures 6a and 6b, we illustrate how errors in

the velocity model for downhole monitoring have the potential to cause both vertical and horizontal location errors. For dual downhole monitoring arrays (frequently encountered in reservoir monitoring), we show that event locations may be located preferentially in the direction perpendicular to the axis of symmetry between the monitoring wells (Figure 7). Again, these roughly linear event groupings may be incorrectly interpreted as induced fracture orientations to the untrained eye. We note, that the main difference between downhole and surface monitoring arises from horizontal layering; the artifacts of the horizontal layering are case specific and should be addressed for specific velocity model. However, operators should be acutely aware of the need for accurate velocity model and should keep a good track of acquired seismic surveys in the vicinity of the monitoring boreholes, such information is frequently lost (especially in the process of property transfers).

Event uncertainties (summarized in Table 1) for surface microseismic monitoring are significant but tend to be well behaved and easily interpreted in comparison to their downhole counterparts. Because of the noisy surface environment associated with reservoir production or fracture stimulation treatments, uncertainties related to traveltimes picks are a significant source of error for events recorded on a surface array. These errors are partially mitigated through the use of a large, redundant array with thousands of receivers. As shown in Figure 5, location uncertainties for microseismic events recorded on a surface array are much more poorly constrained vertically than horizontally. As a general rule, depth estimation from a surface array is not as robust as from a downhole array. This fact becomes particularly apparent when considering depth location errors due to velocity model inaccuracies (Figures 6c and 6d). These sizable velocity related depth errors illustrate the need to carefully calibrate the velocity model using perforation shots early on in the surface microseismic processing workflow. It follows that if the main purpose of a microseismic experiment is to determine the vertical growth pattern of seismicity induced by hydrocarbon production or during hydrofracture stimulation, it may be prudent to use the downhole methodology if possible. However, a significant upside to the surface microseismic methodology is that the lateral location errors are very robust in comparison to downhole techniques. Surface microseismic event

distributions are typically void of many of the systematic geometry induced errors inherent with downhole measurements. If determination of fracture orientation or azimuth in map view is the main objective of a particular microseismic experiment, the surface methodology may be a superior choice. In general, fewer interpretation pitfalls exist for surface microseismic and event distribution in map view is very stable even in light of the possibility of significant velocity and depth related errors.

	Vertical position	Horizontal position	Sensitivity to velocity model
Borehole single vertical array	1-10s of meters for most common scenarios	Significantly better in radial direction, azimuthal uncertainty in 10s of meters	All coordinates are affected (poor vertical, and horizontal)
Surface 2D monitoring array depth:offset = 1:1	Several 10s (40+ m) of meters for most common scenarios	No specific bias in any direction below 10 m for most common scenarios	Vertical position is very sensitive, horizontal position is very robust
Borehole Dual monitoring array	Similar as single monitoring array with good velocity model	Significantly dependent on relative position to the plane of symmetry	Very sensitive and creates artifacts close the plane of symmetry

Table 1: The table below summarizes the uncertainties of event location estimates according to the simulations carried out in this study. For a sensor array in a vertical borehole, uncertainties are lowest in the radial direction from the center of the array to the event location and worst in the azimuthal direction. If the radial direction is split into its vertical and horizontal components, the uncertainty depends on where the event is relative to the array center. If the array straddles the event location the vertical uncertainty is greater than the horizontal while the opposite might be true when the event is location below or above the array

(depending on how far above or below). A two-dimensional sensor array at the surface has gives event locations with relatively low uncertainty in the horizontal plane while the vertical uncertainty is larger. This assumes that the event location is covered by the surface array. Contrary to intuition, using sensor arrays in two vertical boreholes does not necessarily reduce the uncertainty in event location. Uncertainty in the vertical direction is similar to the single borehole case but the horizontal uncertainty strongly depends on the position of the event location relative to the plane of symmetry (a vertical plane that bisects a line between the two wells in map view). Event locations estimated from borehole arrays, either single or dual, are very sensitive to errors in the velocity model. The dual borehole monitoring array is in addition subject to a significant bias that causes event to line up in or around the plane of symmetry. The horizontal uncertainty of event locations obtained from a surface array is robust against velocity errors while the vertical uncertainty is very sensitive to it.

We summarize this study by specific recommendations which should reduce artifacts in microseismic event locations or at least bring these artifacts to the attention of an interpreter. The smallest uncertainty for a location obtained from a single monitoring borehole is achieved for events near the center of the monitoring array. For such an event, a short array gives event locations with larger uncertainties than a long array. For a given array length, the number of sensors has a minor impact. Therefore, for downhole monitoring the array should compass the stimulated reservoir and span approximately the maximum expected event distance. Surface monitoring mostly suffers from the estimation of hypocenter depth. The trade-off between origin time and depth can be reduced by accurate velocity model and small standard deviation of arrival time picks. Therefore, a good calibration shot is essential for both velocity model calibration and reducing arrival time uncertainty.

Recommended literature:

Location from downhole receivers:

Rutledge, J.T., Phillips, W.S., 2003. Hydraulic stimulation of natural fractures as revealed by induced microearthquakes, Carthage Cotton Valley gas field, east Texas. *Geophysics* 68, 441–452.

House, L., 1987. Locating microearthquakes induced by hydraulic fracturing in crystalline rocks, *Geophys. Res. Lett.*, 14(9), 919-921.

Bulant P., Eisner L., Ivan Pšenčík and Joël Le Calvez, 2007. Importance of Borehole Deviation Surveys for Monitoring of Hydraulic Fracturing Treatments. *Geophysical Prospecting*, 55 (6), 891-899.

Velocity model effects:

Vesnaver, A., Lovisa, L. and Böhm, G., 2008: Full 3D relocation of microseisms for reservoir monitoring. *SEG, Expanded Abstracts*, 28

Backazimuth accuracy from downhole receivers:

Fischer, T., Eisner, L., Rutledge, J. 2008: Determination of S-wave slowness from a linear array of borehole receivers. *Geophysical Journal International*, in print.

Drew, J., White, R. , and Wolfe, J., 2008: Microseismic event azimuth estimation: establishing a relationship between hodogram linearity and uncertainty in event azimuth. *SEG, Expanded Abstracts*, 28.

Surface monitoring of microseismic events:

Lakings, J.D., Duncan, P. M., Neale, C. and Theiner, T., 2005: Surface based microseismic monitoring of a hydraulic fracture well stimulation in the Barnett shale *SEG, Expanded Abstracts*, 25 , no. 1, 605-608.

Source mechanisms:

Nolen-Hoeksema, R.C., Ruff, L.J., 2001. Moment tensor inversion of microseisms from the B-sand propped hydrofracture, M-site, Colorado. *Tectonophysics* 336, 163–181.

Jechumtálová, Z., Eisner, L., 2008. Seismic source mechanism inversion from a linear array of receivers reveals non-double-couple seismic events induced by hydraulic fracturing in sedimentary formation. *Tectonophysics* (2008), doi:10.1016/j.tecto.2008.07.011.